Fluorinated oil-surfactant mixtures with the density of water: artificial cells for synthetic biology

Roberto Laos[1,2], Steven Benner[1*]

[1]Foundation for Applied Molecular Evolution, Alachua, Florida, United States of America
Current address: 13709 Progress Blvd. Box 7, Alachua, Florida 32615, United States of America

[2]Panamerican Biolabs LLC
Current address: 7226 NW 52nd Ter. Gainesville Florida 32653, United States of America

* Corresponding author: manuscripts@ffame.org

Abstract

Water-in-oil emulsions provide matrices for compartments that have many uses in diversity science. However, hydrophobic species are frequently incompatible with biological systems. For this reason, fluorinated matrices are often sought, since fluorinated species are neither hydrophilic nor hydrophobic; they therefore do not interact with most biomolecules. However, most fluorinated oils have densities much higher than the density of water (1 g/ml). Consequently, water droplets float in

fluorinated oils, aggregating near their surfaces. This facilitates droplet-droplet collision and fusion, exposing droplets to air interfaces and making their manipulation difficult. Here, we report the synthesis, characterization, and use of fluorinated polysiloxane oils that have densities close to the density of water. These, with a non-ionic fluorosilicone surfactant, produce thermostable water-in-oil emulsions that neither float nor sink. We show how droplets in these emulsions can host many biological processes, including PCR, DNA origami, rolling circle amplification (RCA), and Taqman® assays. Further, oil-diffusible reagents can initiate reactions within the droplets. The droplets can also be used with unnatural DNA emerging from synthetic biology, including DNA built from artificially expanded genetic information systems (AEGIS) with six nucleotide "letters".

Introduction

"Artificial cells"[1] [2] and other compartments have many potential applications in diversity science and nanotechnology, including applications in drug delivery [3-5], , enzyme directed evolution [6, 7] [8, 9] [10] [11], and models for the origin of life [12-16]. While water-hydrophobe-water systems are analogs of natural cells [17] [18] [19-22], simple water-in-oil emulsions are intrinsically easier to assemble and more stable to environmental change (especially heating) as compartment analogs of cells. The contents of each droplet can remain separated from contents of all other droplets.

As with standard cells, compartments can maintain a link between the structures of molecules inside the droplet (the "phenotype") and the structures of the molecules that encode them (the "genotype"). This is important when experimentalists seek to direct the evolution of nucleic acids and their encoded proteins under selective pressure. For

example, compartmentalization in two-phase artificial cell systems has been used for directed evolution [23] in the form of "compartmentalized self replication" (CSR). Developed by Tawfik and Griffiths, CSR holds proteins and genes together in water droplets suspended in oil emulsions [24]. CSR was applied to the directed evolution of DNA polymerases by Holliger and his collaborators [6]. CSR has also been used to select DNA polymerases that accept unnatural nucleotides [8] [25].

Here, droplet technologies and the diversity science that they support intersects with synthetic biology. For example, in one of its many versions, synthetic biologists seek to put alien "xeno" nucleic acids (xNAs) into artificial cells. One example of xNA are artificially expanded genetic information systems (AEGIS) that increase the number of independently replicable nucleotides from 4 to as many as 12. By shuffling hydrogen bonding patterns of the G:C and A:T pairs while retaining their Watson-Crick size-complementarity [26], AEGIS DNA can evolve to produce molecules (AEGISbodies) that bind to liver and breast cancer cells [27], isolated proteins [28], and recombinant cell systems [27]. Several of these are used to deliver drugs to cells in AEGISbody-nanotrain-drug conjugates [29]. Modified nucleic acids can potentially be used as therapeutics [30]; recently some AEGIS components have been suggested as potential inhibitors of the RNA polymerase from SARS-CoV-2 [31].

Despite these applications, useful and robust water-in-oil systems have proven difficult to generate. For example, early water-in-oil systems used Span80® [32] as part of their surfactant system. Span80® is, however, derived from animal fat, which makes this product vary from batch to batch. In our experience, emulsions using Span80® proved

unreliable. Thus, we observed dark precipitates at the bottom of oil phases in Span80®-based mixtures.

Synthetic oils and surfactants can also be problematic. For example, a variety of silicone surfactants are used in cosmetics. Some, commercialized by Degussa (now Evonik), are not available commercially in research-sized amounts. However, some generate dark precipitates as well [33].

Even with stable, available, and reproducible materials, compartment stability becomes an issue. For an emulsion to be useful, it must remain stable over time with respect to droplet-droplet fusion. The key component preventing fusion is a surface-active agent, a surfactant [34]. The surfactant must lower the surface tension of the liquid, stabilize the emulsion, and diminish coalescence [34] [35]. Many hydrophobic surfactants are known. However, hydrophobic surfactants can invade the hydrophobic cores of proteins and other biologics, disrupting their function.

For these and other reasons, some turn to fluorinated oils and surfactants as replacements for hydrocarbon oils and hydrophobic-hydrophilic surfactants. Fluorine forms a third phase that is immiscible with both hydrophilic and hydrophobic phases. "Fluorous" species are sufficiently orthogonal to both hydrophilic and hydrophobic systems as to render them inert with respect to most biomolecules. Thus, fluorinated oils are used for drug delivery [36, 37], blood substitutes [38, 39], and diagnostics [40].

Several fluorinated oils and surfactants are now commercially available for water-oil emulsions, and several of these are widely used.

However, fluorinated matrices generally have densities considerably higher than water. For example, the fluorinated oil HFE-7500 has a density of ~ 1.6 g/mL [41] [42] [43]. Fluorinert® FC40 has a density between 1.845 and 1.895 [44] [45] [46].

In these media, water droplets float. This concentrates droplets at the top of the emulsion. This, in turn, makes the droplets difficult to manipulate in microfluidic devices. Concentration of the droplets in the top of the fluid also increases the number of droplet-droplet encounters, which encourages droplet fusion.

These considerations provided the motivation to seek fluorinated oils that have a density close to 1 g/mL, the density of water droplets in which biological processes act. We report here the synthesis, characterization, and application of such low-density fluorinated oils, as well as surfactants that enable their use.

Materials and methods

Materials

Monomers 1,3,5-trimethyl 1,3,5-tris(3,3,3-trifluoropropyl)cyclotrisiloxane, 2,4,6,8-tetramethylcyclotetrasiloxane, and hexamethylcyclotrisiloxane were purchased from Changzhou Fluoride Chemical Co. Genuine Technology. Hexamethyldisiloxane was purchased from Acros. Amberlyst® 15 hydrogen form and potassium trichloro(ethylene) platinate (II) hydrate were purchased from Sigma-Aldrich.

Amyl nitrite 95.0+% was purchased from TCI. Nonafluorohexyldimethylchlorosilane, and allyloxy(polyethylene oxide) (4-7 EO) were obtained from Gelest. All chemicals were used without purification.

110 For nanostructures, "Folding kit basic p7249 Cuboid with large aperture" was obtained
111 from Tilibit Nanosystems. All natural DNA oligos and fluorescent probes were obtained
112 from IDT. Oligos containing artificial nucleotides, artificial triphosphates dZTP, dPTP
113 and reversible terminator dGTP-ONH_2 were obtained from Firebird Molecular
114 Biosciences. Phi29 polymerase was from New England Biolabs. Eppendorf™ Snap-Cap
115 Microcentrifuge Biopur™ Safe-Lock™ Tubes were from Fisher Scientific. EvaGreen®
116 Dye 20X in water was from Biotium.
117

118 ## Ring-opening polymerization

119 Polysiloxanes were prepared by the ring-opening reaction shown on Fig 1. Two
120 different protocols were used:
121 **Protocol 1.** The fluorinated monomer 1,3,5-trimethyl 1,3,5-tris-(3,3,3-trifluoropropyl)-
122 cyclotrisiloxane (12 g; 25,6 mmol) was mixed with the non-fluorinated monomer
123 hexamethylcyclotrisiloxane (72 g; 323.7 mmol) and hexamethyl disiloxane (3 mL; 14,1
124 mmol); the second acted as a chain terminator. The mixture was heated to 75 °C in an
125 oil bath. Amberlyst® 15 catalyst (1.2 g) was added once the reaction mixture was
126 homogeneous. The reaction proceeded under Ar for 3 hours at 75 °C. Once cooled, the
127 reaction mixture was decanted from the Amberlyst® catalyst.
128 The products were then resolved by distillation under reduced pressure (23 mm Hg) in
129 a Kugelrohr apparatus. Unreacted materials were removed at 90º C; the remaining fluid
130 was labeled Fluid A. A low molecular weight (LMW, Fluid B) fraction was obtained by
131 distillation (150 C, 23 mm Hg); a high molecular weight fraction remained, undistilled
132 (HMW fraction).

The densities of the various fractions were measured using a balance and positive displacement pipette. A glass vial and a pipette tip were placed in a balance and zeroed. Then, fluid (100 μL) was taken into the pipette and the tip was cleaned with a wipe. The liquid and the pipette tip were then placed on the glass vial and weighed again. This was done three times; the average is reported.

Protocol 2. The fluorinated monomer 1,3,5trimethyl 1,3,5-tris(3,3,3-trifluoropropyl) cyclotrisiloxane (25.26 g; 53.9 mmol) was mixed with the non-fluorinated monomer, hexamethylcyclotrisiloxane (36 g; 161.8 mmol) and hexamethyl disiloxane (2.8 mL; 13.11 mmol). The mixture was heated to 75 °C in an oil bath. Catalyst Amberlyst® 15 (1.2 g) was added last, again after the mixture was homogeneous. The reaction proceeded under Ar for 4 hours at 75 °C. Then, the opaque product mixture was decanted to separate the catalyst. Distillation using a Kugelrohr apparatus (90 °C, 26 mm Hg) removed unreacted starting materials. This remaining fluid was left at room temperature for 8 hours, after which it had separate into two layers (top layer: fluid C; bottom layer: fluid D).

Figure 1. Ring-opening polymerization used to produce the fluorosilicone fluid. The two cyclotrisiloxane monomers are reacted along hexamethyl disiloxane, which acts as a chain terminator. The catalyst Amberlyst® 15 acts as an acid catalyst for the ring-opening reaction.

Fluorinated surfactant

Several fluorinated chains and hydrophilic poly(oxyethylene) hydrophiles were synthesized following the work of Kobayashi and Owen [47] (data not shown). The

156 preferred surfactant used in the experiments shown in this manuscript contains the side
157 chain: H_{xf} ($CF_3CF_2CF_2CF_2CH_2CH_2$-). The synthesis of this surfactant is shown in Fig 2.
158
159 **Figure 2.** Synthesis of fluorinated surfactant with the side chain
160 H_{xf} ($CF_3CF_2CF_2CF_2CH_2CH_2$-). Synthesis begins with the hydrolysis of
161 nonafluorohexyldimethylchlorosilane, followed by an equilibrium reaction with
162 hexamethylcyclotrisiloxane in the presence of the acid catalyst Amberlyst® 15 to
163 produce a SiH functional fluorosilicone hydrophobe. The last step is the hydrosilation of
164 the SiH with allyloxy(polyethylene oxide) to produce the fluorosilicone nonionic
165 surfactant.
166

167 Gel permeation chromatography

168 Gel permeation chromatography was performed by Cambridge Polymer Group
169 (Boston, MA) using an Agilent 1100 Series HPLC Gel Permeation Chromatogram
170 equipped with an autosampler, thermostatted column oven, and refractive index
171 detector. The column used for the separation was the Agilent PLgel Mixed-B column (10
172 μm particle size; 300 mm X 7.5 mm) which has a nominal linear molecular weight
173 separation range from 500-10,000,000 g/mol. These columns are packed with a
174 stationary phase consisting of ~10 μm gel particles which are composed of a highly
175 crosslinked polystyrene/divinylbenzene matrix. These columns are organic GPC
176 columns, compatible with most organic mobile phase solvents. One column was
177 considered sufficient for the analysis.

178 Data collected by refractive index (RI) detection was used for characterization of the
179 molecular weight distribution, molecular weight moments, and polydispersity of the
180 samples. The data were analyzed using the Agilent GPC/SEC software v A.02.01. A
181 calibration curve was prepared using polystyrene standards with molecular weights
182 between approximately 500 and 10,000,000 g/mol. A measured amount of the material
183 was transferred to a glass vial with a PTFE lined screw cap. An amount of toluene
184 sufficient to produce a sample concentration of 5 mg/ml was added to each sample,
185 which were then mixed using gentle agitation at a temperature of 30°C overnight. All
186 samples were clear and colorless. The samples were filtered through 0.45 µm PTFE
187 syringe filters into autosampler vials, filled to the shoulder. Three autosampler vials
188 were prepared of the samples for triplicate injection purposes. Molecular weight
189 moments and polydispersity index (PDI) were calculated by Agilent GPC/SEC Software
190 (v A.02.01) as:

191 $Mn = \Sigma MiNi/\Sigma Ni$

192 $Mw = \Sigma Mi2Ni/\Sigma MiNi$

193 $Mz = \Sigma Mi3\ Ni/\Sigma Mi2\ Ni$

194 $PDI = Mw/Mn$

195 Origami DNA

196 The origami folding mixture comprised 208 staples, each 200 nM (Table in S1 Table)
197 and a scaffold (20 nM), which was a single-stranded DNA p7249 isolated from
198 M13mp18 (7249 nucleotides) in Tris buffer (5 mM, pH ~ 8.2, with 1 mM EDTA, 20 mM
199 $MgCl_2$, and 5 mM NaCl.

200 Droplet formation was done using PDMS radial chips that empty droplets of aqueous
201 phase from 20 µm channels into an annular oil flow channel of 50 µm, as previously
202 described by Paegel and Joyce [10]. The continuous phase was Fluid B (see Protocol
203 1) with the fluorinated surfactant 2% (v/v). This was pumped at a rate of 5 µL/min while
204 the aqueous phase was pumped at a rate of 7 µL/min.
205 The origami mixture, both bulk (as a positive control) and emulsified, were placed in a
206 thermal cycler at 65° C for 10 minutes and then cooled to 60° C at 0.1° C/s. After this
207 hold, the temperature was lowered by 0.5° C steps (0.1° C/s rate) and held at the new
208 temperature for 30 minutes until 40° C was reached. At the end of the cooling steps the
209 emulsion was centrifugated for 5 minutes at 5000 x g. Then, 25 µL of the origami
210 reaction were mixed with the provided 6X loading buffer provided with the kit and loaded
211 in an agarose gel 0.5 X Tris-borate EDTA buffer with ethidium bromide and 6 mM
212 $MgCl_2$.
213

214 Six-nucleotide PCR with Artificially Expanded Genetic Information
215 Systems (AEGIS)

216 An aqueous solution holding all components required for a PCR was prepared,
217 consisting of: (a) primers (20 nM each) 5'- GACGGACTGCCTATGAG-3 and 5'-
218 GAGGCGATCGCAGTATC-3'; (b) double stranded template (2 x 10^{-7} µM):
219 5'- GACGGACTGCCTATGAGCAGTT**Z**AAAAG**Z**TATGATACTGCGATCGC CTC-3' and
220 5'- GAGGCGATCGCAGTATCATA**P**CTTTT**P**AACTGCTCATAGGCAGTCCGTC-3'; (c)
221 substrates, dNTPs, dZTP, and dPTP (0.2 mM each), (d) Evagreen 2X; (e) a variant
222 DNA polymerase (Sso7d-Taq(Δ1-280) [R587Q E626K I707L E708K A743H E832G]) at

223 7.1 x 10-2 μM; and (f) buffer, with 20 mM Tris-HCl, pH 8.4; 10 mM $(NH_4)_2SO_4$; 10 mM
224 KCl; 2 mM $MgSO_4$; 0.1% Triton® X-100.
225 The mixture was dispersed into the fluorous oil emulsion at 25°C, again using a
226 PDMS device. As before, the radial chip emptied the aqueous phase from 20 μm
227 channels into an annular oil flow channel of 50 μm [10]. The matrix phase was pumped
228 through the PDMS chip at a rate of 12 μL/min; the aqueous phase was pumped at 5
229 μL/min.
230

231 **Taqman® assay in droplets**

232 An aqueous solution containing the components of a Taqman® assay reaction was
233 prepared to contain:
234 • Template: 5'-CAGCAGTGCCAGCAGAACAAAGGTATTCATCTTAGTGAPGTGCGC
235 AGTCAG CTCACTACT-3', at 0.4 μM concentration.
236 • Primer: 5'-AGTAGTG AGCTGACTGCGC-3', at 0.2 μM concentration.; and
237 • Probe: 5'- FAM-ATGAATACC-ZEN-TTTGTTCTCTGCTGG CAACTGCTG-3'
238 The other components of the reaction mixture were: (a) substrate dNTPs and dZTP,
239 each at 0.2 mM; (b) buffer at 10 mM Tris pH 8.3, 1.5 mM $MgCl_2$, 50 mM KCl; and (c)
240 enzyme, a variant of Taq DNA polymerase [R587Q, E832C], 6 pmol/50 μL reaction.
241 The aqueous mixture (100 μL) was emulsified into fluorinated oil (300 μL) with 2%
242 surfactant (v/v) and a 6 mm stainless steel bead within a Snap-Cap Microcentrifuge
243 Biopur™ Safe-Lock™ Tube. The tube was then fitted in a 96-well storage plate and
244 secured between the top and bottom plates of TissueLyser (Quiagen). The components
245 were then mixed for 10 seconds at 15 Hz followed by 7 seconds at 17 Hz. Then, the

246 emulsion was transferred to PCR tubes with an optically clear lid and placed in the
247 following cycle: 40 x [95° C for 8 seconds; 62° C for 24 seconds] and acquired
248 fluorescence after each cycle using a Lightcycler® 96 (Roche Life Science).
249

250 Rolling circle amplification (RCA) in droplets

251 An aqueous mixture comprising all of the components for a RCA reaction was
252 prepared to include: (a) 1X Phi29 buffer (New England Biolabs), which has 50 mM Tris-
253 HCl at pH 7.5, 10 mM $MgCl_2$, 10 mM $(NH_4)_2SO_4$, and 4 mM DTT (@ 25°C); (b)
254 triphosphates, dATP, dCTP, dTTP 0.2 mM each; (c) a 3'-blocked triphosphate, to
255 prevent premature initiation of the RCA, dGTP-ONH_2 0.2 mM; (d) primer at 0.8 μM,
256 having the sequence 5'-CAGGGCTGGGCATAGAAGTCAGGGCAGA-3'; (e)
257 polymerase, Phi29 0.2 U/μL, with BSA 0.2 μg/μL; and (f) a circular ssDNA template
258 molecule at 0.0985 μM. The circular ssDNA template was prepared by circularizing: P-
259 5'TATGCCCAGCCCTGTA
260 AGATGAAGATAGCGCACAATGGTCGGATTCTCAACTCGTATTCTCAACTCGTAT
261 TCTCAACTCGTCTCTGCCCTGACTTC-3' with Circ ligase (Lucigen) according to the
262 manufacturer protocol.
263 The aqueous mixture holding all the components necessary for RCA (except dGTP)
264 was emulsified by placing 100 μL of the aqueous mixture with 300 μL of fluorinated
265 Fluid C (see Protocol 2), 2% surfactant (v/v), and a 6 mm stainless steel bead in a
266 Snap-Cap Microcentrifuge Biopur™ Safe-Lock™ Tube. The tube was then fitted in a 96-
267 well storage plate and secured between the top and bottom plates of TissueLyser
268 (Quiagen) and then mixed for 10 seconds at 15 Hz followed by 7 seconds at 17 Hz.

269 After the emulsion was formed, 60 µL of the emulsion was mixed with 200 µL of high
270 molecular weight fluid (see Protocol 1) with amyl nitrite (0.1% v/v). The mixture was
271 transferred to PCR tubes with an optical clear lid and placed at 37º C. The amyl nitrite
272 diffused through the fluorous phase, entered the aqueous droplets, and removed the
273 amino group from the dGTP-ONH_2 [48] (Fig 3). This allowed the RCA to continue.
274 Evidence for successful RCA came by measuring fluorescence for 10 seconds after
275 each time interval of 1 minute over a period of 2 hours.
276
277 **Figure 3. Reversible terminator converted to dGTP.** Aminoxy 3'-OH blocked dG
278 triphosphate converted to dGTP with a free OH by reaction with amyl nitrite.
279
280 **Expression and purification of the polymerase variants used here**
281 A plasmid (pJExpress414, DNA 2.0) containing the gene encoding the Taq DNA
282 polymerase variant of interest was expressed in *E. coli* C43(DE3) (37º C, overnight
283 growth, IPTG 0.5 mM) in LB media (50 mL). The next morning, cells were pelleted (~
284 0.75 g) in a refrigerated centrifuge for 10 minutes at 5000 x g and stored at -20º C. The
285 pellet was resuspended in 2.5 mL of Tris 50 mM; glucose 50 mM; EDTA 1 mM; pH 8.0
286 and heat-shocked at 75º C for 10 minutes, then mixed with 3.75 mL of BugBuster®
287 master mix (Novagen) for 20 minutes at room temperature. The lysate was pelleted in
288 1.5 mL tubes, at 21 000 x g for 5 min and the supernatant was mixed with Ni NTA resin
289 (1.5 mL of resuspended resin washed and resuspended in 4 mL of Lysis buffer: Tris
290 HCl, 20 mM pH 8.0; NaCl 500 mM, imidazole 10 mM). The lysate and the resin were
291 then incubated and gently spun at 4º C for 1 h.

292 The lysate was then loaded on a column and washed with: (a) 2 mL wash: Tris, 20
293 mM; NaCl, 1 M; followed by (b) 1 mL wash: Tris, 20 mM; NaCl, 150 mM; followed by (c)
294 2 mL wash: Tris, 20 mM; NaCl, 500 mM; imidazole, 20 mM; and (d) eluted with elution
295 buffer: 1 mL Tris HCl, 10 mM, pH 8.0, NaCl 250 mM, imidazole 500 mM. Buffer was
296 exchanged by ultracentrifugation (AMICON, 15 mL, 50 000 MW cutoff) to final storage
297 buffer, which was 10 mM Tris pH 8.0; 100 mM KCl; 0.5 mM DTT; 0.1 mM EDTA; 0.5
298 %Tween 20; 0.5 % Igepal; glycerol 50%. Protein concentration was measured using
299 Pierce™ BCA Protein Assay Kit, following the manufacturer recommendations.

300 # Results

301 Fluorine has an atomic mass of 19, meaning fluorinated molecules are intrinsically
302 denser than water. However, this greater atomic mass can be partly offset by the larger
303 mean volumes of CF_2 (38 $Å^3$) and CF_3 (92 $Å^3$) groups relative to CH_2 (27 $Å^3$) and CH_3
304 (54 $Å^3$) [31], both less dense than water. Therefore, we reasoned that fluorous oils
305 having a density of water might be obtained by balancing their fluorinated components
306 with alkane components. This balancing must also consider the density of silicon (Si =
307 28 daltons) since cyclotrisiloxanes are part of the polymerization mixture.
308 With these considerations, we explored methods to prepare low-density fluorous oils
309 by reacting siloxanes having both alkane and trifluoromethylalkane side chains,
310 specifically 1,3,5-trimethyl 1,3,5-tris(3,3,3-trifluoropropyl)-cyclotrisiloxane and
311 hexamethylcyclotrisiloxane (Fig 1).
312

313 ## Ring-opening polymerization

314 Acid catalyzed ring-opening polymerization produced a series of polysiloxanes. The
315 addition of hexamethyldisiloxane as a chain terminator prevented the production of
316 species of higher molecular weight, limiting the viscosity of higher molecular weight
317 species; species with very high viscosity are not desired in microfluidics.
318 Polymerization under these conditions produced a fluid with bimodal molecular weight
319 distribution, with a high molecular weight (Mp ~ 9400 g/mol) and a low molecular weight
320 (Mp ~ 300 g/mol). After removing unreacted materials under vacuum (90º C, 23 mm
321 Hg), the two fractions were separated by Kugelrohr distillation. Approximately 15 mL of
322 the fluid consists of a low molecular weight fraction (150º C, 23 mm Hg) having a
323 density of 1.0565 g/mL. The remaining fluid (~ 53 mL) consists of a high molecular
324 weight fraction with density 1.031 g/mL; this remained undistilled up to 200º C at 23 mm
325 Hg).
326 The low molecular weight fraction contains a higher proportion of fluorinated
327 monomers estimated by ^{1}H-NMR. Fig 4A shows the overlay of two gel permeation
328 chromatography runs of the two distinctive fraction mixtures separated by distillation;
329 they show both an unimodal molecular weight distribution of Mp ~ 10320 g/mol for the
330 high molecular weight fraction and Mp ~ 320 g/mol for the low molecular weight fraction.
331 Values of Mp, Mn, Mw, Mz, and PDI values are tabulated in Table 1. Fig 4B shows an
332 overlay of these two fractions and a third sample that corresponds to a similar
333 polymerization reaction where the fractions were not separated by distillation.
334
335 **Figure 4**. **MW distribution overlays for different fluorinated polysiloxanes.** Panel A:
336 The orange line represents the fraction obtained by distillation using a Kugelrohr

apparatus (150º C, 23 mmHg) which exhibits an unimodal molecular weight distribution (Mp ~ 320 g/mol); the purple line represents the remaining material, which exhibits an unimodal molecular weight distribution of Mp ~ 10,320 g/mol. Panel B: Ring-opening polymerization produced a bimodal molecular weight distribution with a high molecular weight peak (Mp ~ 9 400 g/mol) and a low molecular weight peak (Mp ~ 300 g/mol). The high molecular weight and low molecular weight fractions obtained by distillation from a similar reaction are overlapped for comparison. Panel C: Ring-opening polymerization using a higher proportion of fluorinated monomers produced two fluids that spontaneously separated in two layers: The top layer, labeled as Fluid C with a density of 1.0457 g/mL (green line) and the bottom layer labeled as Fluid D (red line) with a density of 1.1347 g/mL. Both fluids showed a bimodal distribution of molecular weights.

Table 1. Summary of molecular weight moments and polydispersity.

sample	Mp [g/mol]	Mn [g/mol]	Mw [g/mol]	Mz [g/mol]	PDI
Fluid A	9404 ± 57.7	1748 ± 31.2	10126 ± 83.5	23 432 ± 415.9	5.793 ± 0.058
Fluid A peak 1	10321 ± 34.6	3,206 ± 486	11,478 ± 74.0	23,241 ± 1,767	3.637 ± 0.561
Fluid A peak 2	321 ± 2.08	230 ± 2.65	305 ± 2.00	375 ± 1.15	1.326 ± 0.008
Fluid C	6412 ± 64	2064 ± 11	6266 ± 116	11521 ± 532	3.04 ± 0.06
Fluid C peak 1	6412 ± 64	4549 ± 34	7529 ± 144	11729 ± 538	1.66 ± 0.019
Fluid C peak 2	626 ± 6	597 ± 3	637 ± 3	674 ± 4	1.07 ± 0.008
Fluid D	645 ± 4	1722 ± 12	6543 ± 119	13708 ± 1289	3.80 ± 0.07
Fluid D peak 1	7178 ± 47	4892 ± 23	8522 ± 70	13426 ± 250	1.74 ± 0.009
Fluid D peak 2	645 ± 4	611 ± 4	661 ± 4	706 ± 4	1.08 ± 0.003

Values reported in polystyrene equivalents for samples: Fluid A peak 1 is referred as high molecular weight fraction (HMW) and Fluid A peak 2 referred as low molecular weight fraction (LMW).

352

353 **Figure 5. ^{1}NMR analysis of fluorosilicone polysiloxanes.** A. Overlay of the ^{1}HNMR
354 of the low molecular weight and the high molecular weight fraction samples indicating
355 the assigned peaks. B. Magnification of the overlay. C. ^{1}HNMR of the low molecular
356 weight fraction showing peak integration. D. ^{1}HNMR of the high molecular weight
357 fraction showing peak integration.

358

359 **^{1}HNMR analysis**

360 Resonances with chemical shifts between 0.0 and 0.3 ppm were assigned to Si-CH_3
361 (labeled "a" in Fig 5A). These signals arise from both fluorinated and non-fluorinated
362 monomers. Resonances with chemical shifts between 0.7 and 0.9 ppm were assigned
363 to the methylene groups attached to Si (α-CH_2-, labeled "b" in Fig 6A). Resonances with
364 chemical shifts between 1.9 and 2.2 ppm were assigned to the methylene beta to the Si
365 (β-CH_2-, labeled '"c" in Fig 6A) for the fluorinated monomers that contained -CH_2^{α}-CH_2^{β}-
366 CF_3.

367

368 The ratios of non-fluorinated monomer to fluorinated monomer were calculated using
369 the integrals from the β protons (denoted by "c") and the Si-CH_3 protons (denoted by
370 "a"). The following equation was used to determine the monomer ratio:

371

372 $$\frac{\text{Non} - \text{fluorinated monomer}}{\text{Fluorinated monomer}} = \frac{(\text{Aa} - 3)/6}{\text{Ac}/2}$$

373

374 Here, A_c is the integration area of the peak for the β-CH_2- protons and A_a is the

375 integration area of the peak for the Si-CH_3 protons. The integration values and

376 monomer ratios are summarized in Table 2.

377

378 **Table 2. Integration of peaks used for determination of the ratio of non-fluorinated**

379 **monomer:fluorinated monomer.**

sample	β-CH_2	Si-CH_3	non-fluorinated monomer: fluorinated monomer
Fluid A peak 2 (LMW)	2	18.3	2.6 : 1
Fluid A peak 1 (HMW)	2	96.3	15.6 : 1

380 Values for samples HMW: high molecular weight and LMW: low molecular weight.

381

382

383

384 **Table 3. Viscosity, density and other properties measured on fluorinated polysiloxanes.**

density g/mL	Viscosity* (Centistokes)	^{1}HNMR β–CH_2 integral	^{1}HNMR Si-CH_3 integral	Mw	PDI	non-fluorinated monomer: fluorinated monomer
1.0310	n/d	2	18.3	305	1.3	2.55 : 1
1.0565	n/d	2	96.3	11 478	3.6	15.55 : 1
1.0593	4.1	2	18.11	n/d	n/d	2.51 : 1
1.0763	4.3	2	15.02	n/d	n/d	2.00 : 1
1.1397	4.5	2	11.48	n/d	n/d	1.41 : 1
0.986	67	2	58	10 126	5.8	9.17 : 1
1.0457	6.06	2	33.98	6 266	3.04	5.16 : 1
1.1347	10.8	2	12.24	6 543	3.8	1.54 : 1

385 *Average viscosity is reported using a Newtonian model. Determined by Cambridge Polymer Group
386 using a TA Instruments DHR-2 rheometer.
387
388 The integral of the resonances assigned to the Si-CH_3 units (0.0 to 0.3 ppm) is
389 inversely proportional to the fraction of fluorinated monomers present in the fluid. Higher
390 content of fluorinated monomers also correlates with lower viscosity values and higher
391 densities (Table 3). We found that the nonionic fluorinated surfactant shown is soluble
392 up to 5% in the low molecular weight fraction while it is not soluble in the high molecular
393 weight fraction. We found useful to combine four volumes of the high molecular weight
394 fraction with 1 volume of the low molecular weight fraction obtained using protocol 1.
395 Using one particular batch 4 mL of a HMW fraction (density: 0.984 g/mL) was combined
396 with 1 mL of the LMW fraction (density: 1.0613 g/mL) to produce a fluid of density 1.009
397 g/mol where we could solubilize 2% of the fluorinated surfactant without visible
398 separation of the surfactant from the fluid.
399 The preferred oils were then challenged to support processes that involve both DNA
400 and enzymes, all useful in biomolecular sciences, nanotechnology, and diversity
401 science:
402 (a) Assembly of origami DNA nanostructures inside droplets suspended in the
403 fluorinated oil.
404 (b) PCR amplification of a 6-letter DNA templates inside droplets suspended in the
405 fluorinated oil, including those built from an AEGIS DNA alphabet.
406 (c) Generation of fluorescent signals inside droplets suspended in the fluorinated oil
407 using a Taqman® assay, also with six-letter DNA real-time PCR.

408 (d) Generation of fluorescent signals inside droplets suspended in the fluorinated oil
409 using blocked nucleoside triphosphate's, where the reaction is initiated by adding a
410 reagent (amyl nitrite) that is able to diffuse through the fluorinated, enter the droplet, and
411 remove the blocking group.

412 ## Origami DNA

413 An origami kit obtained from Tilibit Nanosystems that assembles to form a cuboid of
414 dimensions 61 nm x 8 nm x 52 nm with an aperture of 9 nm x 15 nm was set up as
415 suggested by the manufacturer. The formation of the nanostructure was verified by its
416 distinctive shift in migration of the scaffold/staples mixture when electrophoresed in an
417 agarose gel in 0.5 X TBE with ethidium bromide and 6 mM $MgCl_2$. It was observed (Fig
418 6) that both the emulsified and non-emulsified origami reaction gave the expected
419 nanostructure without noticeable difference. The result shown in Fig 6 comes from
420 droplets prepared using microfluidics as described in the experimental section. This
421 experiment was repeated preparing the emulsions using a Tiussuelyser (Quiagen)
422 without noticeable difference between the methods of emulsification (data not shown).
423

424 **Figure 6. DNA electrophoresis in agarose (2%) showing the formation of origami**
425 **structures in droplets.** The gel was 0.5 X Tris-borate EDTA buffer with ethidium
426 bromide and 6 mM $MgCl_2$. The “nanostructure PF-2, cuboid with large aperture” origami
427 structure (Tilibit Nanosystems). The scaffold is a single-stranded DNA type p7249
428 isolated from M13mp18 of length 7249 bases. The staples are a mixture of 208 oligos.
429 Scaffold runs near the 2000 bp MW marker. A sample of the mixture of scaffold and
430 staples not annealed is run for comparison. The origami folded properly shows a

431 distinctive migration on the gel. Annealing was done by incubating at 65° C for 10
432 minutes then cooled down from 60° C to 40 ° C at a rate of 1° C per hour.
433

434 AEGIS PCR with 6-Letters

435 To demonstrate that droplets suspended in the iso-dense fluorinated oil had thermal
436 stability adequate to support PCR and, in particular, PCR containing AEGIS bases, a
437 double stranded DNA molecule with 49 bp containing the AEGIS pair Z:P (Fig 7) was
438 used as template. The enzyme used to amplify this was a derivative of the Taq DNA
439 polymerase where the amino acids 1-280 were deleted (removing the exonuclease
440 domain), with the N-terminus of the catalytic domain fused to a processivity enhancing
441 domain from *Sulfolobus solfataricus*. The Taq variant was selected using diversity
442 science, and has 6 mutations, two specific for enhancing the incorporation of the pair
443 Z:P. The enzyme is described as: Sso7d-Taq (Δ 1-280) R587Q E626K I707L E708K
444 A743H E832G.
445 Progress of the PCR was monitored by observing the fluorescence of Evagreen®,
446 which intercalates into double-stranded PCR amplicons. Fig 7 shows real time PCR
447 fluorescence signals arising from a PCR done, as a control, in bulk aqueous solution, a
448 positive control. Fig 7 also shows real time PCR fluorescence signals arising from a
449 PCR done in parallel in water droplets emulsified in iso-dense fluorinated oil. The Ct
450 values (the number of cycles needed to reach a threshold) for both the bulk PCR and
451 the emulsified PCR were substantially the same. This establishes the value of these
452 emulsions in PCR.

453 Quantitiative, in the emulsified PCR, the final "plateau" fluorescent signal was about
454 one third of the signal observed with the bulk PCR. This is consistent with the fact that
455 the active volume of the bulk (unemulsified) PCR was ca. three times the volume of the
456 active volume in the emulsified PCR. These results showed that neither the surfactant
457 nor the fluorinated oil had any measurable impact on the progress of the PCR. This is
458 consistent with the orthogonality of the fluorinated oil and the surfactant with respect all
459 biological molecules involved in the PCR.
460
461 **Figure 7.** Real time PCR showing emergence of fluorescence from interacalated
462 Evagreen® without emulsification (blue line) and in the emulsified PCR (red line). The
463 emulsion was prepared using microfluidic devices made of PDMS. The aqueous phase
464 was delivered (25°C) at 5 µL/min by the PDMS chip into the fluorinated oil matrix at 12
465 µL/min. The matrix phase is a fluorinated silicon polymer with 2% of surfactant (see Figs
466 1 and 2 for structures). The buffer was 20 mM Tris-HCl pH 8.4; 10 mM $(NH_4)_2SO_4$; 10
467 mM KCl; 2 mM $MgSO_4$; 0.1% Triton® X-100;. Primers are 0.02 µM; template 2 x 10^{-7}
468 µM; dNTPs both natural and AEGIS 0.2 mM; Evagreen 2X; polymerase at 7.1 x 10^{-2}
469 was: Sso7d-Taq (Δ 1-280) R587Q E626K I707L E708K A743H E832G
470

471 Taqman® assay

472 One standard way to detect DNA is a Taqman® assay. Here, DNA polymerase from
473 *Thermus aquaticus* degrades the downstream strand using its 5'-3' exonuclease activity
474 displacing a probe from the template, cleaving the probe in the process. This cleavage

475 separates a fluorescent reporter (here, fluorescein, FAM) from one end of the probe
476 from a fluorescence quencher at the other end of the probe, to give a fluorescent signal.
477 Here, we adapted the Taqman® assay to detect a target analyte that contained AEGIS
478 dZ and dP. As before, the aqueous phase was emulsified by mixing 100 µL of aqueous
479 phase mixed with 300 µL of fluorinated oil (1 volume of LMW fraction and 4 volumes of
480 the HMW fraction, see protocol 1) with 2% of surfactant shown on Fig 2. Emulsions
481 were made by shaking using a QUIAGEN TissueLyser II (15 Hz for 10 seconds followed
482 by 17 Hz for 7 seconds) in a Snap-Cap Microcentrifuge Biopur™ Safe-Lock™ tubes
483 containing a 6 mm stainless steel bead.
484 Fig 9 shows in real-time fluorescence detected in that assay. Again, output was
485 essentially the same as observed in bulk Taqman® assays. This again showed the
486 orthogonality of the iso-dense fluorinated oil-fluorinated surfactant system. The Taq
487 DNA polymerase variant used contains two mutations (R587Q, E832C) that favor the
488 incorporation of the Z:P pair
489
490 **Figure 8. Taqman® assay in droplets.** Top: Scheme of the Taqman® assay containing
491 AEGIS (dZ:dP pair hydrogen bonding shown). Bottom: Real-time fluorescence detected
492 from FAM probe when Taq [R587Q E832C] polymerase places a dZ opposite dP. The
493 blue line is the fluorescence from a non-emulsified reaction. The red line corresponds to
494 the signal from the emulsified reaction. The emulsion was made by mixing 100 µL of
495 aqueous phase with 300 µL of a fluorinated oil with 2% (v/v) fluorinated surfactant as
496 shown on Fig 2. Mixed in Quiagen TissueLyser II in the presence of a 6 mm stainless

497 steel bead at 15 Hz for 10 seconds followed by 17 Hz for 7 seconds using a Snap-Cap
498 Microcentrifuge Biopur™ Safe-Lock™ Tube containing a stainless steel ball.
499

500 RCA in droplets

501 Many regard water droplets in compartments as inaccessible to reagent-based
502 manipulation. Here, we overcame this limitation by showing that reactions can be
503 initiated within droplets isolated in fluorinated oil by adding "turn on" reagents that can
504 diffuse through the oil. This allowed us to mix DNA templates, DNA primers,
505 triphosphates and enzymes without having any RCA before the material was
506 encapsulated in emulsions.
507 To enable this controlled chemistry, we exploited the aminoxy group in a 3'-blocked
508 nucleoside triphosphate. With a 3'-O-NH_2 blocking group, primers cannot be extended
509 by a DNA polymerase. However, treatment with amyl nitrite cleaves the O-N bond to
510 yield an extendable 3'-OH group. Further, we discovered that amyl nitrite will diffuse
511 through the fluorinated oil and partition into the aqueous droplets. There, it cleaves the
512 O-N bond to allow primer extension to occur.
513 This manipulative architecture was demonstrated using rolling circle amplification
514 (RCA). RCA works by having a circular template, a primer that binds to that circular
515 template, and a strand displacing polymerase that extends that primer, displacing
516 already synthesized DNA as it proceeds around the circle. Here, the aqueous phase
517 used to prepare the droplets contains a circularized template 96 nucleotides around, a
518 primer complementary to the circular template, and three natural dNTPs (dATP, dCTP

519 and dTTP). To prevent the RCA from proceeding during emulsification, dGTP carried a
520 3'-aminoxy block, dGTP-ONH_2. The polymerase was Phi29 DNA polymerase.
521 RCA was initiated by contacting the emulsion (60 µL) with 200 µL of a high molecular
522 weight fraction of the fluorinated oil containing amyl nitrite (0.1% v/v). The progress of
523 the RCA was followed by measuring fluorescence emitted by an intercalating fluor
524 (EvaGreen®) in a Light Cycler over a period of 2-3 hours (Fig 9). These data showed
525 the successful O-N bond cleavage and RCA product formation.
526
527 **Figure 9. Amplification curves obtained using the LightCycler96 for RCA**
528 **amplification in droplets.** Fluorescence detection is acquired after each two step cycle
529 [37 C for 60 seconds- 37 C for10 seconds followed by aquisition] x 99 cycles. This lasts
530 about 2 hours. Line A: Emulsion using all natural dNTPs. No initiator needed, or added.
531 Line B: Emulsion using all natural dNTPs. Initiator added to 0.08%. Line C. Emulsion
532 containing dATP, dCTP, dTTP and dGTP-ONH^2. Initiator added to 0.077%.
533 Line D: Emulsion containing dATP, dCTP, dTTP and dGTP-ONH^2. No amyl nitrite "turn
534 on" reagent added.
535

536 # Discussion

537 The growing interest in synthetic cells [49] matches a growing interest in engineering
538 enzymes for synthetic biology [50, 51] [52] by directed evolution. For example, Tawfik
539 and Griffiths [24] developed a method to link genotype and phenotype in droplets of
540 water emulsified in oil called "Compartmentalized Self-Replication" (CSR). This strategy

541 was adapted in the Holliger laboratory for the directed evolution of DNA polymerases
542 [6].
543 However, various laboratories have reported difficulties in reproducing CSR
544 procedures. One of the first problems identified was associated to the surfactant Span
545 80® [53]. It is very likely that Span 80®, which is derived from animal fat, carries in
546 uncontrolled amounts a problematic contaminant. Indeed the Holliger group reports the
547 need for an antioxidant to avoid oxidation due to peroxide contaminants in Span 80®
548 [32]. Thus, while results are possible with surfactant mixtures containing Span 80®,
549 these are hit-or-miss, and this corner of biotechnology has become known in the
550 community as problematically irreproducible. Further, although they are not frequently
551 published, many observations suggest that some biological systems suffer denaturation
552 when they encounter hydrocarbon oils, causing CSR to fail.
553 For this reason, many have turned to the synthetic materials and a third liquid phase,
554 the "fluorous phase". Kobayashi and Owen reported some time ago the synthesis of
555 non-ionic fluorosilicone surfactants with 3,3,3-trifluoropropyl and 3,3,4,4,5,5,6,6,6-
556 nonafluorohexyl side chains with poly(oxyethylene) hydrophiles [47]. We synthesized
557 and tested some of these and found that the highest solubility and thermal stability of
558 the emulsions formed was achieved was between a fluorinated polysiloxane with
559 particular characteristics and a fluorinated surfactant with a fluorinated side chain Hxf
560 ($CF_3CF_2CF_2CF_2CH_2CH_2$-) (Fig 2).
561 Here, balancing the mixture of hydrocarbon-carrying silanes, intrinsically less dense
562 than water, with fluorohydrocarbon-carrying silanes, intrinsically more dense than water,
563 yielded mixtures that had the density essentially identical to the density of water. As the

564 density of water can change with different amounts of solutes, the density of the
565 fluorinated oils described here can be changed to match that density.
566 Multiple standard challenges in nanotechnology were applied to these iso-dense
567 fluorinated oil-surfactant systems: (a) origami, (b) PCR, (c) Taqman® assays, and (d)
568 RCA. All of these biochemical reactions worked as well in these iso-dense fluorinated
569 oil-surfactant systems as their non-emulsified analogs. Thus, they add a significant and
570 important new resource for nanotechnology and diversity science.

571 Acknowledgments

572 We thank Tamara Aigner and Jean-Philippe Sobczak from Tilibit Nanosystems for
573 useful discussions and assistance in troubleshooting and confirming the formation of the
574 origami structure. We thank Brian Paegel laboratory for providing molds and assistance
575 in preparing microfluidic devices as well as valuable discussions in surfactant design.

576 References

577 1. Buddingh BC, van Hest JCM. Artificial Cells: Synthetic Compartments with Life-like
578 Functionality and Adaptivity. Accounts of Chemical Research. 2017;50(4):769-77. doi:
579 10.1021/acs.accounts.6b00512. PubMed PMID: WOS:000399859800013.
580 2. Elani Y. Interfacing Living and Synthetic Cells as an Emerging Frontier in Synthetic
581 Biology. Angewandte Chemie-International Edition. 2020. doi: 10.1002/anie.202006941.
582 PubMed PMID: WOS:000578742300001.

583 3. Akbarzadeh A, Rezaei-Sadabady R, Davaran S, Joo SW, Zarghami N, Hanifehpour Y, et al.
584 Liposome: classification, preparation, and applications. Nanoscale Research Letters. 2013;8.
585 doi: 10.1186/1556-276x-8-102. PubMed PMID: WOS:000316359300001.
586 4. Allen TM, Cullis PR. Liposomal drug delivery systems: From concept to clinical
587 applications. Advanced Drug Delivery Reviews. 2013;65(1):36-48. doi:
588 10.1016/j.addr.2012.09.037. PubMed PMID: WOS:000315547400008.
589 5. Lammers T, Kiessling F, Hennink WE, Storm G. Drug targeting to tumors: Principles,
590 pitfalls and (pre-) clinical progress. Journal of Controlled Release. 2012;161(2):175-87. doi:
591 10.1016/j.jconrel.2011.09.063. PubMed PMID: WOS:000305790300004.
592 6. Ghadessy FJ, Ong JL, Holliger P. Directed evolution of polymerase function by
593 compartmentalized self-replication. Proc Natl Acad Sci U S A. 2001;98(8):4552-7. doi:
594 10.1073/pnas.071052198. PubMed PMID: PMC31872.
595 7. Ghadessy FJ, Ramsay N, Boudsocq F, Loakes D, Brown A, Iwai S, et al. Generic expansion
596 of the substrate spectrum of a DNA polymerase by directed evolution. Nature Biotechnology.
597 2004;22(6):755-9. doi: 10.1038/nbt974. PubMed PMID: WOS:000221785300038.
598 8. Laos R, Shaw R, Leal NA, Gaucher E, Benner S. Directed Evolution of Polymerases To
599 Accept Nucleotides with Nonstandard Hydrogen Bond Patterns. Biochemistry.
600 2013;52(31):5288-94. doi: 10.1021/bi400558c. PubMed PMID: WOS:000323013700017.
601 9. Laos R, Thomson JM, Benner SA. DNA Polymerases Engineered by Directed Evolution to
602 Incorporate Nonstandard Nucleotides. Frontiers in Microbiology. 2014;5. doi:
603 10.3389/fmicb.2014.00565.

604 10. Paegel BM, Joyce GF. Microfluidic Compartmentalized Directed Evolution. Chemistry &
605 Biology. 2010;17(7):717-24. doi: 10.1016/j.chembiol.2010.05.021. PubMed PMID:
606 WOS:000280831100008.
607 11. Yang JH, Tu R, Yuan HL, Wang QH, Zhu LL. Recent advances in droplet microfluidics for
608 enzyme and cell factory engineering. Critical Reviews in Biotechnology. doi:
609 10.1080/07388551.2021.1898326. PubMed PMID: WOS:000630753400001.
610 12. Kurihara K, Tamura M, Shohda K-i, Toyota T, Suzuki K, Sugawara T. Self-reproduction of
611 supramolecular giant vesicles combined with the amplification of encapsulated DNA. Nat Chem.
612 2011;3(10):775-81. doi: 10.1038/nchem.1127. PubMed PMID: WOS:000295157200010.
613 13. Luisi PL, Walde P, Oberholzer T. Lipid vesicles as possible intermediates in the origin of
614 life. Current Opinion in Colloid & Interface Science. 1999;4(1):33-9. doi: 10.1016/s1359-
615 0294(99)00012-6. PubMed PMID: WOS:000080941800005.
616 14. Stano P. Minimal cells: Relevance and interplay of physical and biochemical factors.
617 Biotechnology Journal. 2011;6(7):850-9. doi: 10.1002/biot.201100079. PubMed PMID:
618 WOS:000292738100009.
619 15. Walde P, Ichikawa S. Enzymes inside lipid vesicles: Preparation, reactivity and
620 applications. Biomolecular Engineering. 2001;18(4):143-77. doi: 10.1016/s1389-0344(01)00088-
621 0. PubMed PMID: WOS:000171578700001.
622 16. Caschera F, Noireaux V. Integration of biological parts toward the synthesis of a minimal
623 cell. Current Opinion in Chemical Biology. 2014;22:85-91. doi: 10.1016/j.cbpa.2014.09.028.
624 PubMed PMID: WOS:000345604000014.

625 17. Huang Y, Kim S-H, Arriaga LR. Emulsion templated vesicles with symmetric or
626 asymmetric membranes. Advances in Colloid and Interface Science. 2017;247:413-25. doi:
627 10.1016/j.cis.2017.07.013. PubMed PMID: WOS:000412150100026.
628 18. Kamiya K, Takeuchi S. Giant liposome formation toward the synthesis of well-defined
629 artificial cells. Journal of Materials Chemistry B. 2017;5(30):5911-23. doi: 10.1039/c7tb01322a.
630 PubMed PMID: WOS:000407083800001.
631 19. Matosevic S. Synthesizing artificial cells from giant unilamellar vesicles: State-of-the art
632 in the development of microfluidic technology. Bioessays. 2012;34(11):992-1001. doi:
633 10.1002/bies.201200105. PubMed PMID: WOS:000309910400015.
634 20. Supramaniam P, Ces O, Salehi-Reyhani A. Microfluidics for Artificial Life: Techniques for
635 Bottom-Up Synthetic Biology. Micromachines. 2019;10(5). doi: 10.3390/mi10050299. PubMed
636 PMID: WOS:000470966700022.
637 21. Trantidou T, Friddin MS, Salehi-Reyhani A, Ces O, Elani Y. Droplet microfluidics for the
638 construction of compartmentalised model membranes. Lab on a Chip. 2018;18(17):2488-509.
639 doi: 10.1039/c8lc00028j. PubMed PMID: WOS:000443279400001.
640 22. van Swaay D, deMello A. Microfluidic methods for forming liposomes. Lab on a Chip.
641 2013;13(5):752-67. doi: 10.1039/c2lc41121k. PubMed PMID: WOS:000314651000001.
642 23. Laos R, Shaw RW, Benner SA. Engineered DNA Polymerases. In: Murakami KS, Trakselis
643 MA, editors. Nucleic Acid Polymerases. Nucleic Acids and Molecular Biology. 302014. p. 163-87.
644 24. Tawfik DS, Griffiths AD. Man-made cell-like compartments for molecular evolution.
645 Nature Biotechnology. 1998;16(7):652-6. doi: 10.1038/nbt0798-652. PubMed PMID:
646 WOS:000074521800029.

647 25. Singh I, Laos R, Hoshika S, Benner SA, Georgiadis MM. Snapshots of an evolved DNA
648 polymerase pre- and post-incorporation of an unnatural nucleotide. Nucleic Acids Research.
649 2018;46(15):7977-88. doi: 10.1093/nar/gky552. PubMed PMID: WOS:000444148100043.
650 26. Benner SA, Karalkar NB, Hoshika S, Laos R, Shaw RW, Matsuura M, et al. Alternative
651 Watson-Crick Synthetic Genetic Systems. Cold Spring Harbor Perspectives in Biology.
652 2016;8(11):26. doi: 10.1101/cshperspect.a023770. PubMed PMID: WOS:000389841300005.
653 27. Zhang LQ, Yang ZY, Trinh TL, Teng IT, Wang S, Bradley KM, et al. Aptamers against Cells
654 Overexpressing Glypican 3 from Expanded Genetic Systems Combined with Cell Engineering and
655 Laboratory Evolution. Angewandte Chemie-International Edition. 2016;55(40):12372-5. doi:
656 10.1002/anie.201605058. PubMed PMID: WOS:000384713700041.
657 28. Biondi E, Lane JD, Das D, Dasgupta S, Piccirilli JA, Hoshika S, et al. Laboratory evolution
658 of artificially expanded DNA gives redesignable aptamers that target the toxic form of anthrax
659 protective antigen. Nucleic Acids Research. 2016;44(20):9565-77. doi: 10.1093/nar/gkw890.
660 PubMed PMID: WOS:000393817800011.
661 29. Zhu GZ, Zheng J, Song EQ, Donovan M, Zhang KJ, Liu C, et al. Self-assembled, aptamer-
662 tethered DNA nanotrains for targeted transport of molecular drugs in cancer theranostics. Proc
663 Natl Acad Sci U S A. 2013;110(20):7998-8003. doi: 10.1073/pnas.1220817110. PubMed PMID:
664 WOS:000319803500016.
665 30. Duffy K, Arangundy-Franklin S, Holliger P. Modified nucleic acids: replication, evolution,
666 and next-generation therapeutics. Bmc Biology. 2020;18(1). doi: 10.1186/s12915-020-00803-6.
667 PubMed PMID: WOS:000568198200001.

668 31. Jena NR, Pant S, Srivastava HK. Artificially expanded genetic information systems
669 (AEGISs) as potent inhibitors of the RNA-dependent RNA polymerase of the SARS-CoV-2.
670 Journal of Biomolecular Structure & Dynamics. 2021:17. doi: 10.1080/07391102.2021.1883112.
671 PubMed PMID: WOS:000616859200001.
672 32. Ramsay N, Jemth A-S, Brown A, Crampton N, Dear P, Holliger P. CyDNA: Synthesis and
673 Replication of Highly Cy-Dye Substituted DNA by an Evolved Polymerase. Journal of the
674 American Chemical Society. 2010;132(14):5096-104. doi: 10.1021/ja909180c. PubMed PMID:
675 WOS:000276553700036.
676 33. Diehl F, Li M, He YP, Kinzler KW, Vogelstein B, Dressman D. BEAMing: single-molecule
677 PCR on microparticles in water-in-oil emulsions. Nature Methods. 2006;3(7):551-9. doi:
678 10.1038/nmeth898. PubMed PMID: WOS:000238669600018.
679 34. Baret JC. Surfactants in droplet-based microfluidics. Lab on a Chip. 2012;12(3):422-33.
680 doi: 10.1039/c1lc20582j. PubMed PMID: WOS:000298964300003.
681 35. Dai B, Leal LG. The mechanism of surfactant effects on drop coalescence. Physics of
682 Fluids. 2008;20(4). doi: 10.1063/1.2911700. PubMed PMID: WOS:000255456600012.
683 36. Riess JG. Fluorous micro- and nanophases with a biomedical perspective. Tetrahedron.
684 2002;58(20):4113-31. doi: 10.1016/s0040-4020(02)00262-4. PubMed PMID:
685 WOS:000175612700037.
686 37. Riess JG. Fluorocarbon-based injectable gaseous microbubbles for diagnosis and
687 therapy. Current Opinion in Colloid & Interface Science. 2003;8(3):259-66. doi: 10.1016/s1359-
688 0294(03)00047-5. PubMed PMID: WOS:000184757000008.

689 38. Riess JG. Fluorocarbon-based oxygen-delivery: Basic principles and product
690 development. Blood Substitutes: Principles, Methods, Products and Clinical Trials, Vol 2.
691 1998:101-26. PubMed PMID: CCC:000072284300006.
692 39. Riess JG. Oxygen carriers ("blood substitutes") - Raison d'Etre, chemistry, and some
693 physiology. Chemical Reviews. 2001;101(9):2797-919. doi: 10.1021/cr970143c. PubMed PMID:
694 WOS:000171047000007.
695 40. Schutt EG, Klein DH, Mattrey RM, Riess JG. Injectable microbubbles as contrast agents
696 for diagnostic ultrasound imaging: The key role of perfluorochemicals. Angewandte Chemie-
697 International Edition. 2003;42(28):3218-35. doi: 10.1002/anie.200200550. PubMed PMID:
698 WOS:000184465000003.
699 41. Abate AR, Weitz DA. High-Order Multiple Emulsions Formed in Poly(dimethylsiloxane)
700 Microfluidics. Small. 2009;5(18):2030-2. doi: 10.1002/smll.200900569. PubMed PMID:
701 WOS:000270342500001.
702 42. Granieri L, Baret JC, Griffiths AD, Merten CA. High-Throughput Screening of Enzymes by
703 Retroviral Display Using Droplet-Based Microfluidics. Chemistry & Biology. 2010;17(3):229-35.
704 doi: 10.1016/j.chembiol.2010.02.011. PubMed PMID: WOS:000276680200005.
705 43. Mazutis L, Araghi AF, Miller OJ, Baret JC, Frenz L, Janoshazi A, et al. Droplet-Based
706 Microfluidic Systems for High-Throughput Single DNA Molecule Isothermal Amplification and
707 Analysis. Analytical Chemistry. 2009;81(12):4813-21. doi: 10.1021/ac900403z. PubMed PMID:
708 WOS:000266969700019.

709 44. Fidalgo LM, Abell C, Huck WTS. Surface-induced droplet fusion in microfluidic devices.
710 Lab on a Chip. 2007;7(8):984-6. doi: 10.1039/b708091c. PubMed PMID:
711 WOS:000248281600013.
712 45. Marcoux PR, Dupoy M, Mathey R, Novelli-Rousseau A, Heran V, Morales S, et al. Micro-
713 confinement of bacteria into w/o emulsion droplets for rapid detection and enumeration.
714 Colloids and Surfaces a-Physicochemical and Engineering Aspects. 2011;377(1-3):54-62. doi:
715 10.1016/j.colsurfa.2010.12.013. PubMed PMID: WOS:000288773900007.
716 46. Schonbrun E, Abate AR, Steinvurzel PE, Weitz DA, Crozier KB. High-throughput
717 fluorescence detection using an integrated zone-plate array. Lab on a Chip. 2010;10(7):852-6.
718 doi: 10.1039/b923554j. PubMed PMID: WOS:000275757600010.
719 47. Kobayashi H, Owen MJ. Nonionic Fluorosilicone Surfactants. Journal of Colloid and
720 Interface Science. 1993;156(2):415-9. doi: 10.1006/jcis.1993.1131. PubMed PMID:
721 WOS:A1993KT88300023.
722 48. Hutter D, Kim MJ, Karalkar N, Leal NA, Chen F, Guggenheim E, et al. Labeled nucleoside
723 triphosphates with reversibly terminating aminoalkoxyl groups. Nucleosides Nucleotides &
724 Nucleic Acids. 2010;29(11-12):879-95. doi: 10.1080/15257770.2010.536191. PubMed PMID:
725 WOS:000284889700008.
726 49. Nie P, Bai Y, Hui M. Synthetic Life with Alternative Nucleic Acids as Genetic Materials.
727 Molecules. 2020;25(15):3483. doi: http://dx.doi.org/10.3390/molecules25153483. PubMed
728 PMID: 2430552638.

729 50. Nikoomanzar A, Chim N, Yik EJ, Chaput JC. Engineering polymerases for applications in
730 synthetic biology. Quarterly Reviews of Biophysics. 2020;53. doi: 10.1017/s0033583520000050.
731 PubMed PMID: WOS:000552696100001.
732 51. Ouaray Z, Singh I, Georgiadis MM, Richards NGJ. Building better enzymes: Molecular
733 basis of improved non-natural nucleobase incorporation by an evolved DNA polymerase.
734 Protein Science. 2020;29(2):455-68. doi: 10.1002/pro.3762. PubMed PMID:
735 WOS:000496314100001.
736 52. Coulther TA, Stern HR, Beuning PJ. Engineering Polymerases for New Functions. Trends
737 in Biotechnology. 2019;37(10):1091-103. doi: 10.1016/j.tibtech.2019.03.011. PubMed PMID:
738 WOS:000485189600009.
739 53. R. L. Directed evolution of polymerases to accept nucleotides with non-strandard
740 hydrogen bonding patterns. Florida, USA: University of Florida; 2015.
741

742 # Supporting information

743 S1 Table 1. List of oligos used as staples in Origami DNA folding experiment.

744

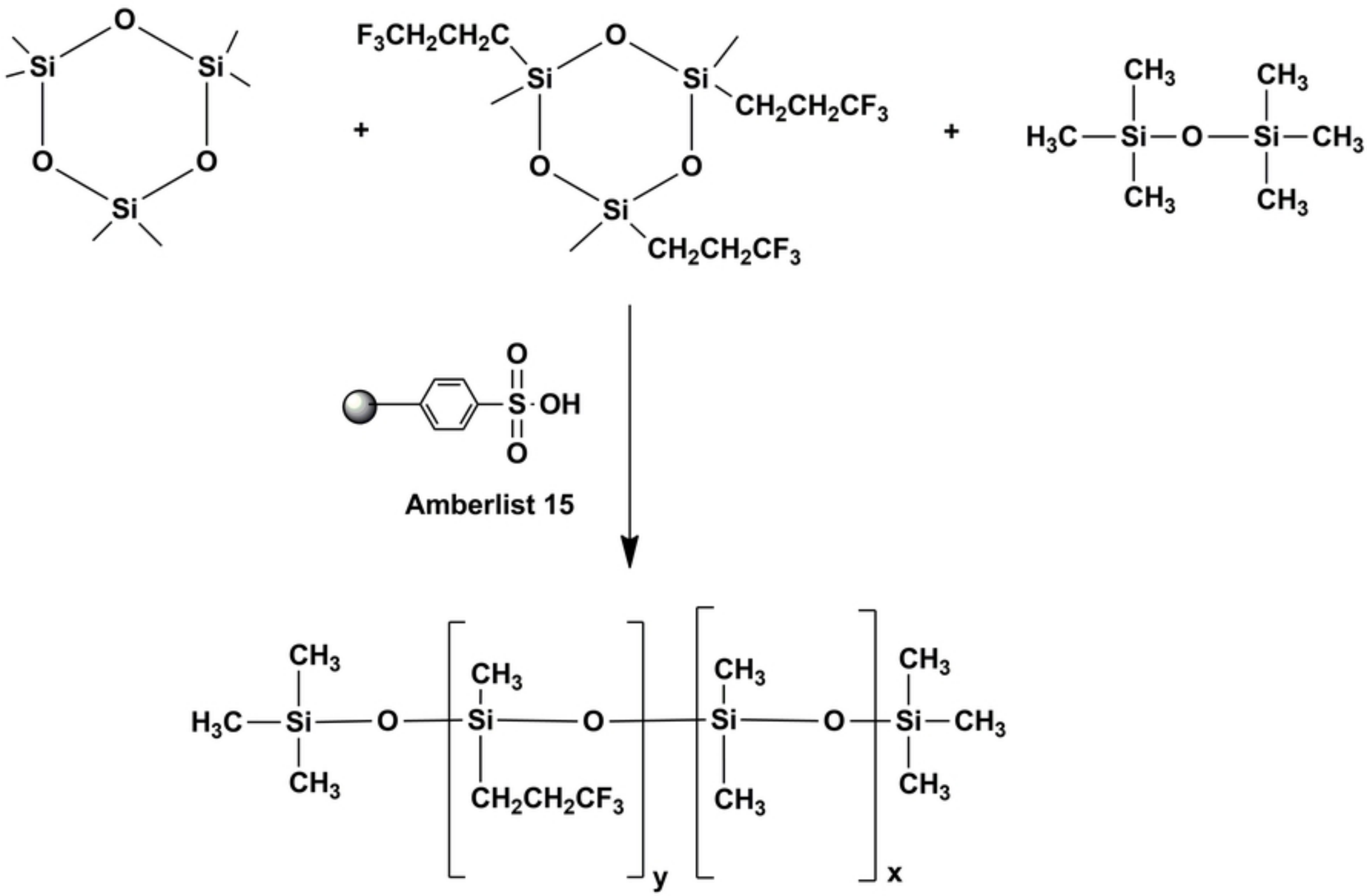

Figure 1

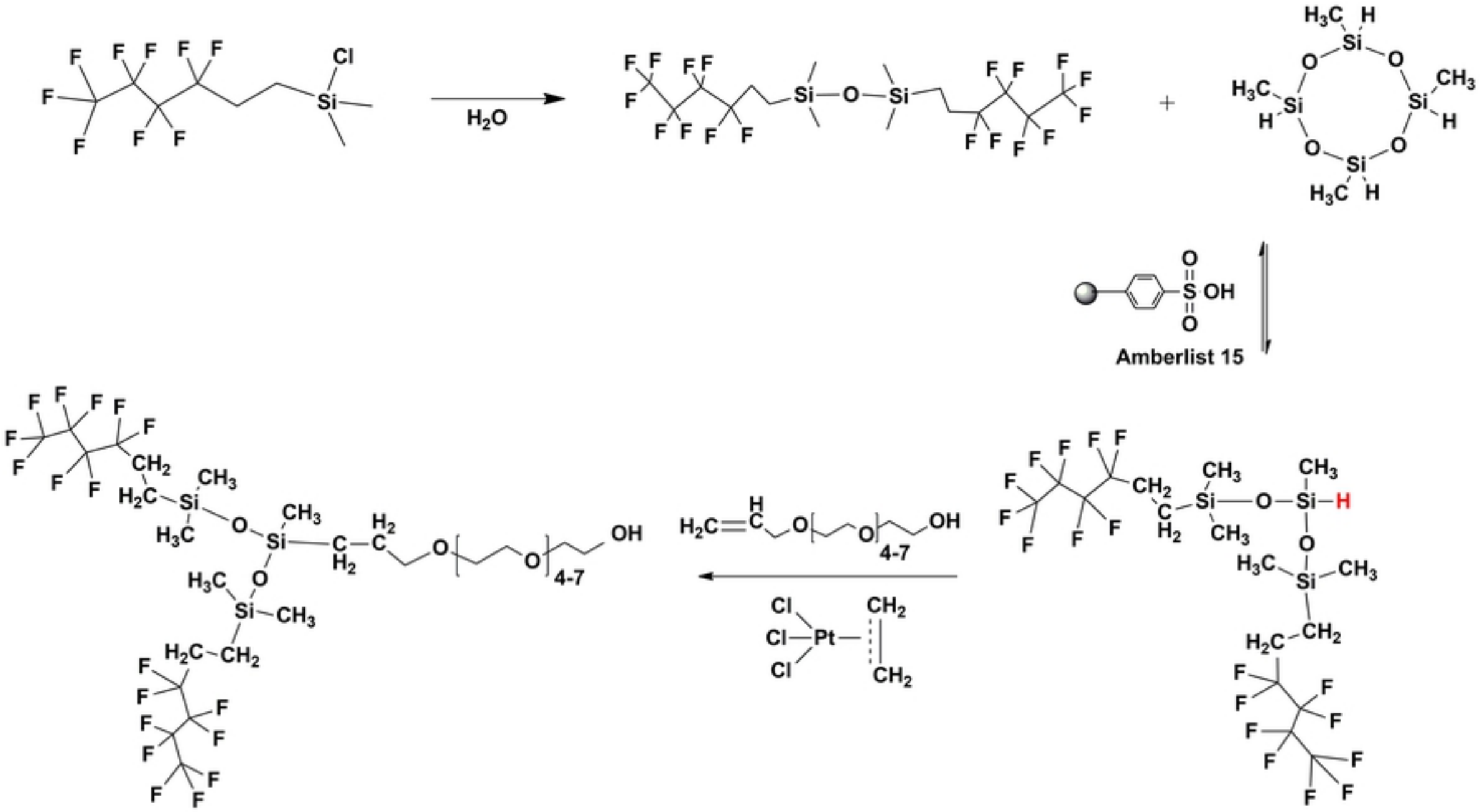

Figure 2

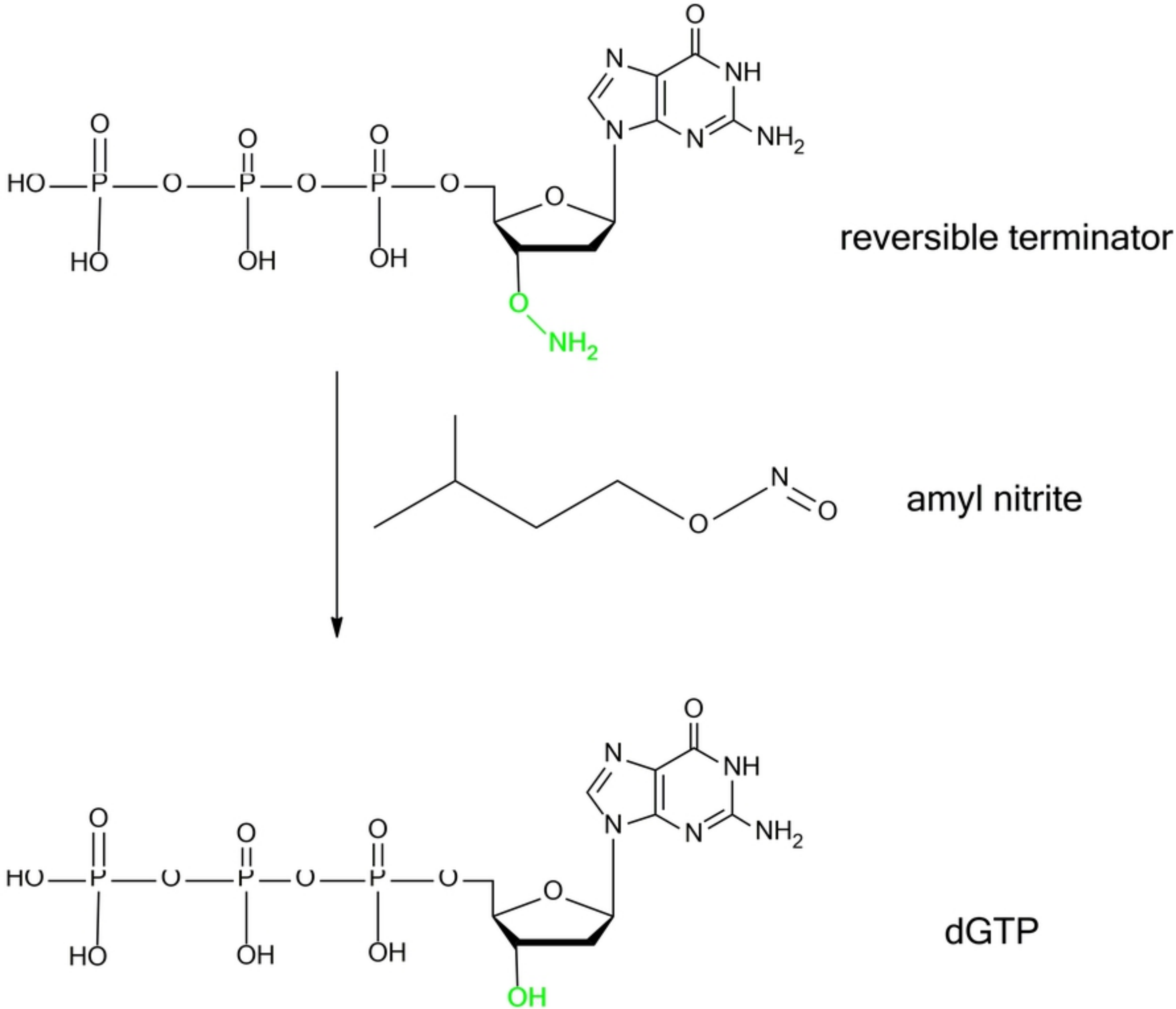

Figure 3

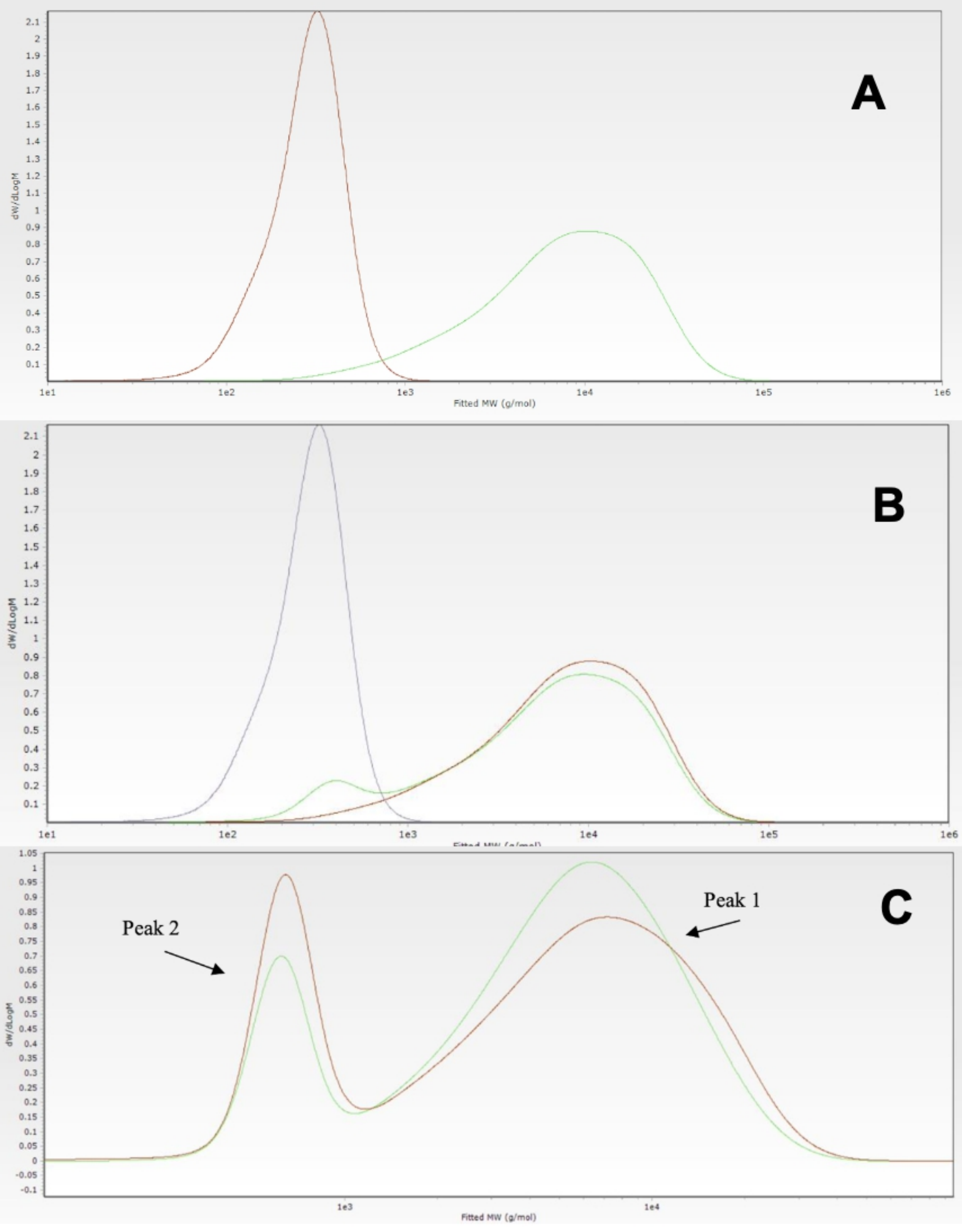

Figure 4

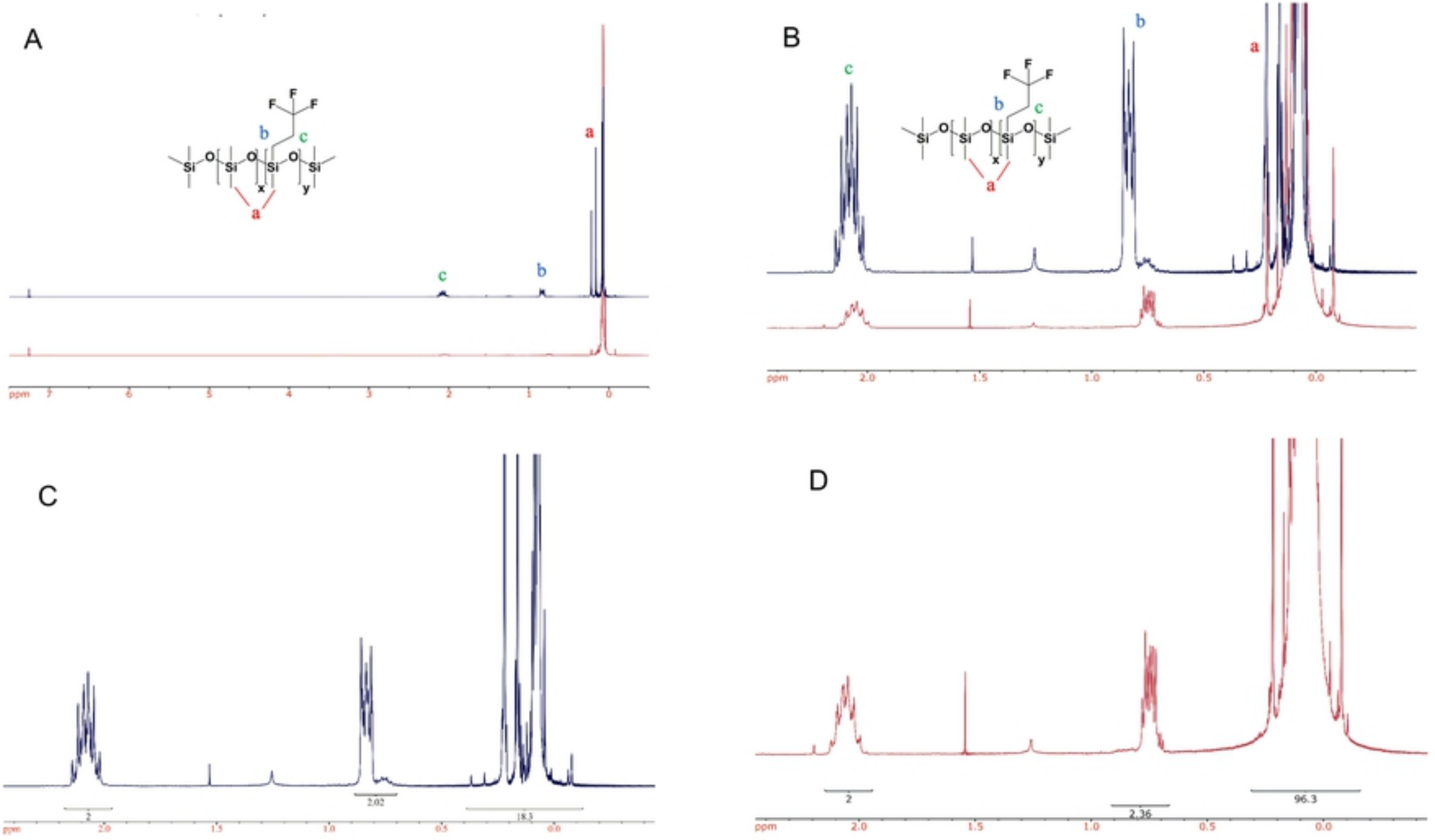

Figure 5

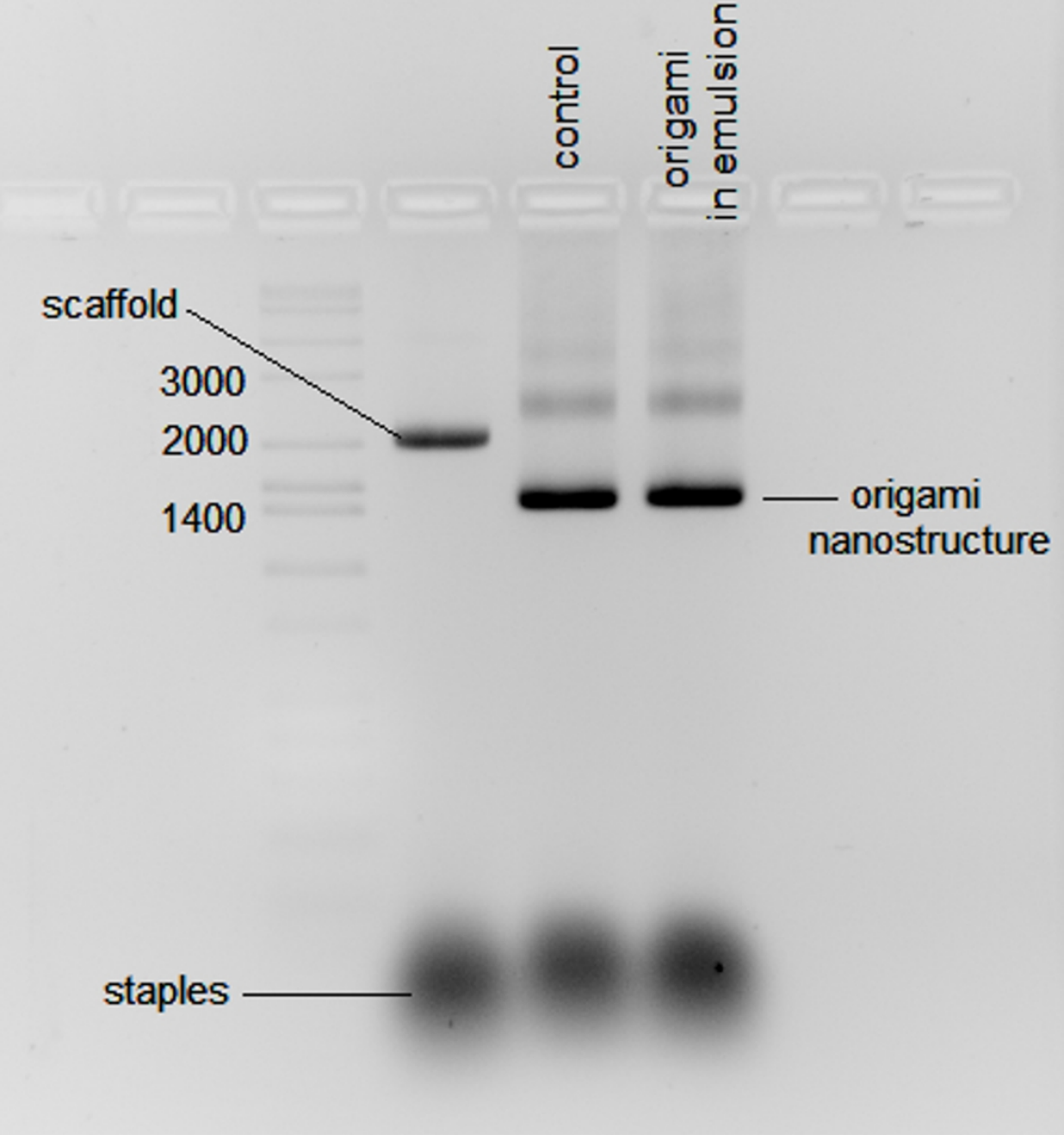
control
origami
in emulsion
scaffold
3000
2000
1400
origami
nanostructure
staples

Figure 6

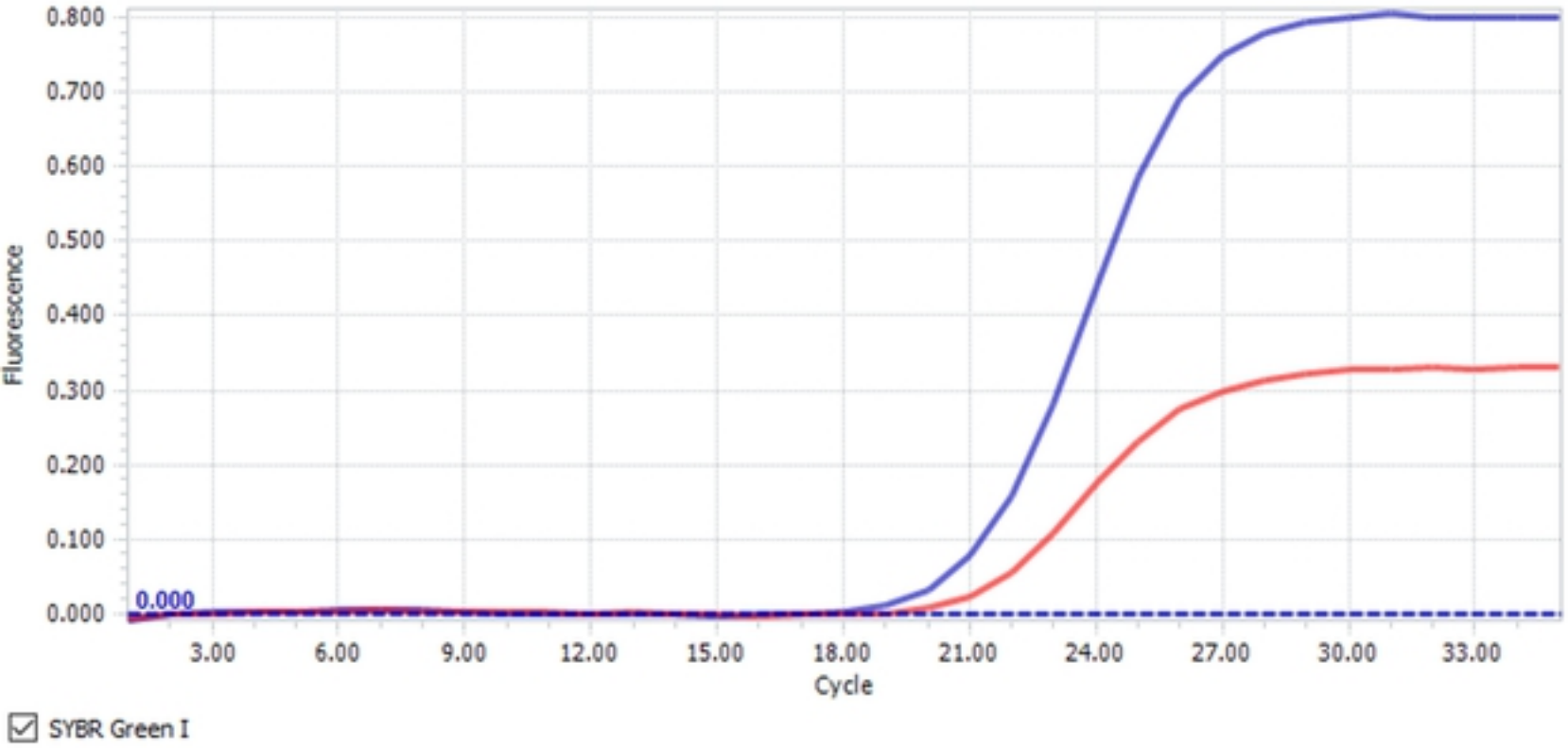

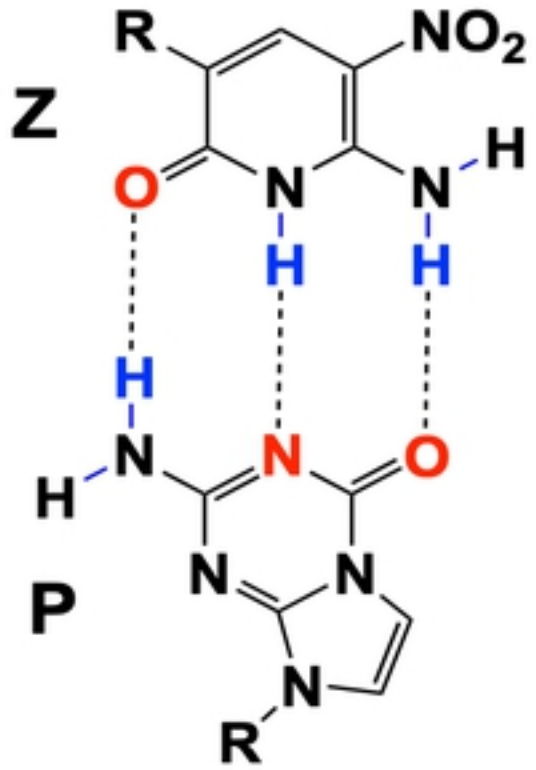


```
                Fwd
5'- GAC GGA CTG CCT ATG AGCAG TTZAAA AGZT A TGA TAC TGC GAT CGC CTC-3'
3'- CTG CCT GAC GGA TAC TCGTC AAPTTT TCPA T ACT ATG ACG CTA GCG GAG-5'
                                                      Rev
```

Figure 7

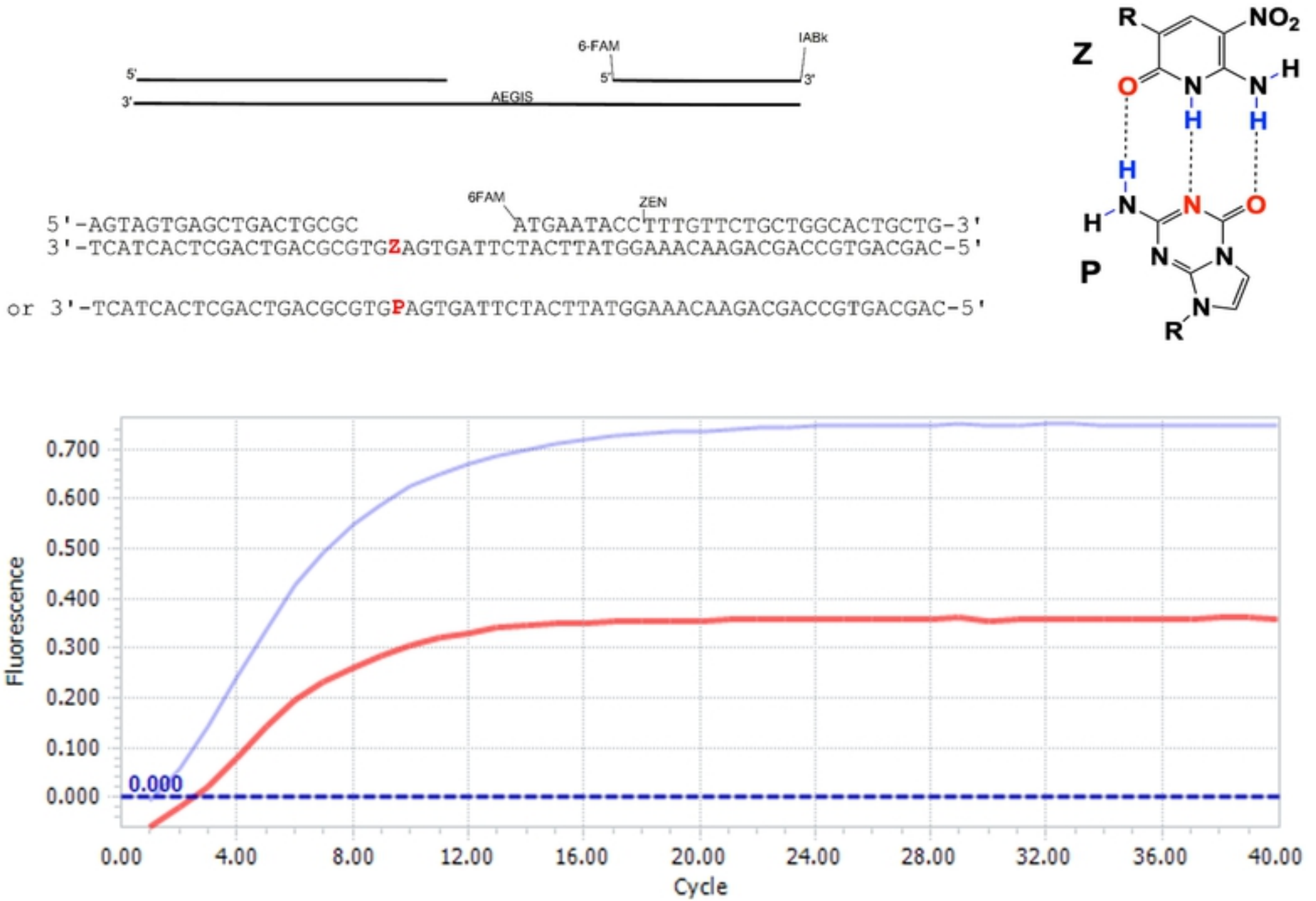
6-FAM
IABk
5'
5'
3'
3'
AEGIS
6FAM
ZEN
5'-AGTAGTGAGCTGACTGCGC ATGAATACCTTTGTTCTGCTGGCACTGCTG-3'
3'-TCATCACTCGACTGACGCGTGZAGTGATTCTACTTATGGAAACAAGACGACCGTGACGAC-5'
or 3'-TCATCACTCGACTGACGCGTGPAGTGATTCTACTTATGGAAACAAGACGACCGTGACGAC-5'
Z
P
R
NO2
O
N
H
Fluorescence
0.700
0.600
0.500
0.400
0.300
0.200
0.100
0.000
0.000
0.00
4.00
8.00
12.00
16.00
20.00
24.00
28.00
32.00
36.00
40.00
Cycle

Figure 8

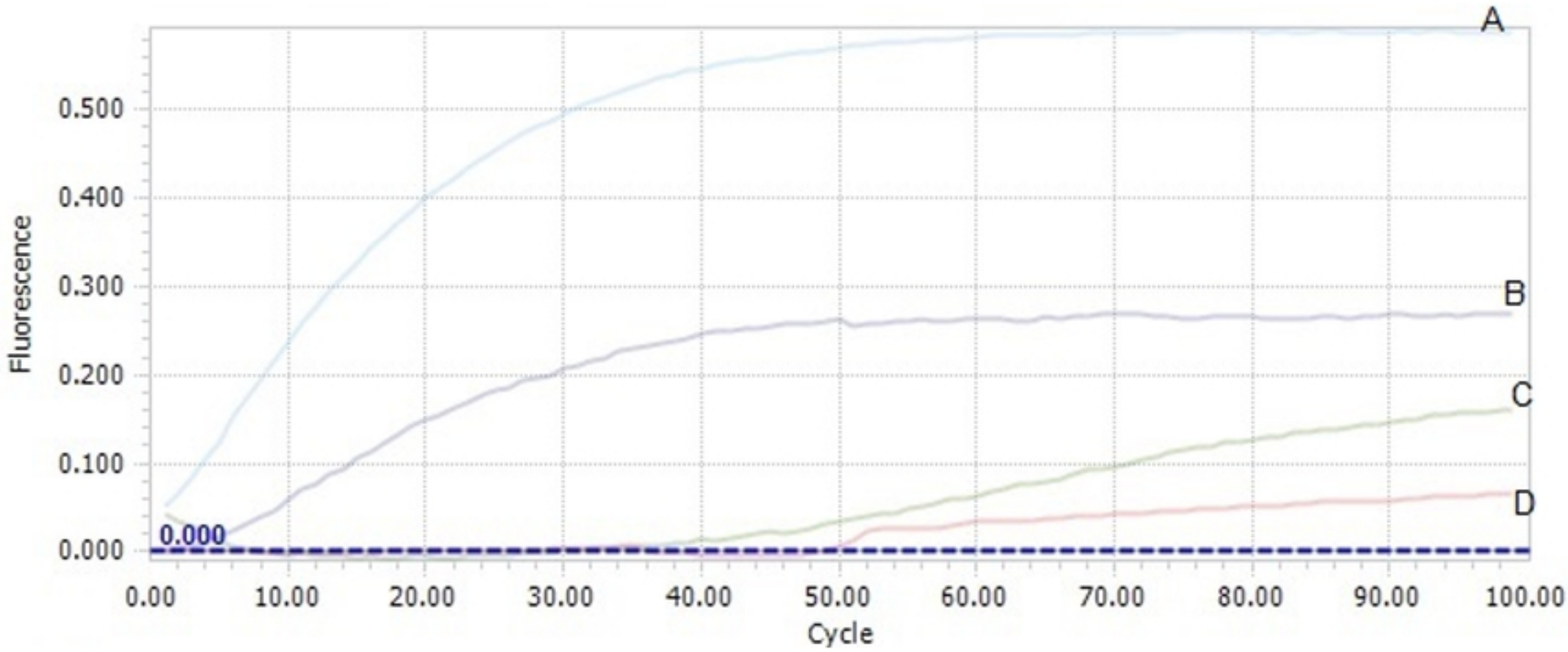
A
B
C
D
0.000
0.500
0.400
0.300
0.200
0.100
0.000
Fluorescence
0.00
10.00
20.00
30.00
40.00
50.00
60.00
70.00
80.00
90.00
100.00
Cycle

Figure 9